that constitute the primary visual cortex (V1) in the mouse, namely, areas 17, 18a and 18b [5, 36, 48, 55]. Area 17 contains one complete representation of the contralateral visual hemifield with the zero vertical meridian represented close to the borders with area 18a (located laterally to area 17), and with gradually more peripheral vertical meridians represented more medially toward the border with area 18b [8, 24, 48, 55, 59]. The binocular zone of the mouse visual cortex occupies approximately the lateral one-third of area 17 and can be distinguished histologically from its higher acetylcholinesterase activity than the other areas [1]. Furthermore, a small (about 10°) part of the ipsilateral hemifield is represented in a small region of area 17 between the representation of the zero vertical meridian and the border with area 18a [8, 12, 55]. About 70% of cells recorded from the binocular segment of V1 respond to appropriate visual stimuli presented via either eye [8, 9, 31]. Even though mice do not have anatomically distinct ocular dominance (OD) columns, they have a critical period during their early postnatal life in which the relative representations of the two eyes in the binocular region of the visual cortex are sensitive to monocular deprivation (MD) [1, 9, 12]. The temporary closure of one eye for MD results in an overall strengthening of the open-eye representation in the visual cortex. Various techniques have been developed to determine OD in the mouse visual cortex by single unit recording [9, 12, 20], recording of visually evoked potentials [11, 22, 39, 46], optical imaging [3, 18, 21], calcium imaging with two-photon microscopy [34, 43, 50], and gene expression analysis of activity-regulated genes, such as *c-fos* [37] or *Arc* [51], in histological sections.

In this review, we summarize our recently reported findings of studies using our novel BAC Tg mouse strain to monitor the neuronal-activity-dependent *Arc-Luc* expression in the mouse visual cortex using bioluminescence signals [23] and compare our mouse strain with other *Arc* reporter mouse strains.

2. NEURONAL IMMEDIATE-EARLY GENE *ARC*

The activity-regulated cytoskeleton-associated protein gene (*Arc*, also known as *Arg3.1*) was first identified as an immediate early gene induced by seizure and depolarization in hippocampal neurons [27, 28]. Hippocampal *Arc* transcripts in rodents are also induced during exploration of a novel environment [14, 17, 54], and the levels of *Arc* expression correlate with learning in hippocampus-dependent spatial learning tasks [16]. Furthermore,

the decrease in the expression level of Arc following infusion of antisense oligonucleotides into the rat hippocampus [15] or the targeted deletion of *Arc* in the mouse [38] interferes with hippocampus-dependent synaptic plasticity and learning and memory. One of the proposed roles of Arc in the regulation of synaptic plasticity is its involvement in α-amino-3-hydroxy-5-methyl-4-isoxazole propionic acid (AMPA)-type glutamate receptor endocytosis [7, 44, 47]. Regulatory mechanisms of *Arc* expression are extensively studied [35].

In the visual cortex, *Arc* expression is induced by light exposure and is used for the mapping of neuronal activity [25, 51]. A study using *Arc* knockout (KO) mice revealed the functions of Arc in the orientation specificity of visual cortical neurons [57]. Furthermore, Arc is suggested to be required in experience-dependent processes that normally establish and modify synaptic connections in the visual cortex [30].

From these studies, *in vivo* monitoring of Arc expression is useful for the analysis of physiological conditions in the brain. However, most of the methods for Arc detection in the above-mentioned studies are *in situ* hybridization and immunohistochemical analysis applied to fixed brain sections. Recently, three research groups have reported the successful *in vivo* imaging of *Arc* expression under physiological and pathological conditions using fluorescent protein gene probes. These probes are the d2-type enhanced green fluorescent protein (EGFP) gene (*d2EGFP*) knocked into the *Arc* locus in mice [57], the fluorescent protein reporter gene *Venus* linked to the 7.1 kbp promoter region of *Arc* in conventional transgenic (Tg) mice [10], and the short-life form of *EGFP, d4EGFP,* introduced into BAC containing *Arc* in BAC Tg mice [13]. Wang et al. [57] successfully monitored Arc expression at the single neuron level from cortical layers II to IV during visual cortical activation using visual stimuli. The two research groups obtained superficial brain fluorescence signals of Venus and d4EGFP from the visual cortex and somatosensory cortex [10, 13] with some autofluorescence noise. These groups could not detect changes in signal intensity associated with experience-dependent plasticity.

3. GENERATION OF NOVEL MOUSE STRAIN TO DETECT EXPRESSION OF *ARC*

One of the powerful *in vivo* imaging probes is luciferase (Luc). Bioluminescence signals emitted from Luc provide a much higher sensitivity

than fluorescence signals for noninvasive detection *in vivo* [2] and are nontoxic, allowing continuous and repeated recording over a long period [29]. Moreover, bioluminescence signals can be detected from the depths of the brain with a very high signal-to-noise (S/N) ratio [40, 45]. These properties of bioluminescence imaging are suitable for the neuroimaging of contextually relevant spatiotemporal expression of Arc in mice. Recently, we have generated and reported on a novel BAC Tg mouse strain to monitor the neuronal-activity-dependent *Arc-Luc* expression using bioluminescence signals [23]. Using the *Arc-Luc* Tg mice, we successfully detected massive plastic changes in bioluminescence signal intensity in the adult mouse visual cortex after visual deprivation.

To generate the Tg mouse strain, we first obtained the mouse BAC clone RP24-388I10 carrying a 221-kbp insert containing the entire *Arc* from the BACPAC Resources Center CHORI. The BAC clone contained the entire *Arc* and about 83 kbp of the 5' upstream sequence and about 125 kbp of the 3' downstream sequence. We introduced *Luc* at the translational initiation site of *Arc* by homologous recombination in *E. coli.* to generate the BAC transgene construct pTg-Arc-Luc (Figure 1).

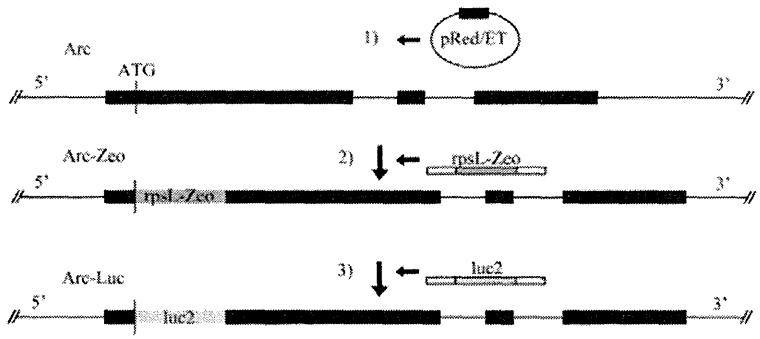

Figure 1. Generation of *Arc-Luc* BAC transgene by homologous recombination in *E. coli.* Steps of homologous recombination in *E. coli* to generate Arc-Luc BAC transgene. First, the Red/ET recombination proteins expression plasmid is introduced into *E. coli* containing Arc BAC DNA. Second, the PCR fragment containing the drug selection cassette (rspL-Zeo) attached with ~50 bps homologous regions at each end is introduced. Third, the DNA fragment containing the luciferase coding region (Luc) attached with about 300 bps homologous regions of Arc at each end is transformed. These steps of homologous recombination are confirmed on the basis of the resistance of *E. coli* to antibiotics, PCR, and Southern blot analysis results, and DNA sequencing.

After the purification of pTg-Arc-Luc DNA, the transgene was linearized by *Not*I digestion, and purified BAC DNA was microinjected into pronuclei of fertilized one-cell embryos from C57BL/6 mice.

Among 49 candidates, we identified 10 lines of mice carrying the *Arc-Luc* transgene by PCR and Southern blot analyses of genomic DNA prepared from tail biopsy specimens. The integrated *Arc-Luc* transgene was stably transmitted to the next generation and one of the lines with strong bioluminescence signals was used for the bioluminescence imaging study.

4. Bioluminescence Imaging of Arc Expression in the Visual Cortex

The Tg mice were anesthetized by sodium pentobarbital injection or inhalation of isoflurane before and during imaging. Because the black fur of the C57BL/6 strain attenuates photon emission, the fur on the head of mice was shaved. The mice were injected with luciferin, a substrate of luciferase under anesthesia. Ten minutes after the luciferin injection, the bioluminescence signal intensity in *Arc-Luc* Tg mice was measured using an *in vivo* imaging system consisting of a dark chamber and a cooled charge-coupled device (CCD) camera. Bioluminescence images were taken for 30 or 180 sec with 4 x 4 binning without using an optical filter. Pseudocolored luminescent images representing the spatial distribution of emitted photons were overlaid on photographs of mice taken in the chamber under a dim light.

To detect light-induced bioluminescence signal intensity changes in the visual cortex, the *Arc-Luc* mice were anesthetized with sodium pentobarbital, and bioluminescence signal intensity was measured for 180 sec. For quantitative analysis, we set a template image of the bioluminescence signals of the brain of each mouse placed under light condition, then the regions of interest (ROIs), including the somatosensory and visual cortex areas, were selected as follows. Using the bioluminescence signal image of the cerebral hemisphere, we defined the long axis and formed a circle with its center in the middle of the long axis and with a radius of 2 mm for the region containing the somatosensory cortex. Similarly, we formed another circle with a radius of 2 mm and with its center located at 1/4 of the length of the long axis from the edge of the caudal border of a bioluminescence signal image to define the ROI containing the visual cortex, as shown in Figure 2. The photon counts in the central regions containing the somatosensory cortex and posterior regions

containing the visual cortex ranged from 8219 to 24044 and from 7080 to 20953, respectively. The photon counts in the central regions and posterior regions of Tg mice under normal light condition were highly correlated (γ = 0.989, n = 32).

In all the experiments, background bioluminescence signal intensity was measured in wild-type (WT) mice injected with luciferin and the *Arc-Luc* Tg mice injected with phosphate-buffered saline (PBS) instead of luciferin. The obtained background bioluminescence signal intensity was subtracted from measured bioluminescence signal intensity. Data were expressed as the mean number of counted photons in the ROI. Bioluminescence signal intensity was calculated from bioluminescence images by ROI analysis using NIH ImageJ.

Using a cooled CCD camera, we detected bioluminescence signals in the nose and head regions of the Tg mice in a dark chamber (Figure 2). Strong signals were detected in the cerebral cortical areas of the brain. To determine the source of the detected bioluminescence signals, we prepared coronal brain slices from the *Arc-Luc* Tg mice and incubated them with luciferin. We detected bioluminescence signals in the cerebral cortex and hippocampus in the brain slices. We were unable to detect any significant bioluminescence signal in other brain regions. These distribution patterns of bioluminescence signals were similar to those reported for *Arc* mRNA in the mouse brain [51].

We further examined the localization of endogenous Arc and exogenous Luc proteins in the *Arc-Luc* Tg mouse brain by double immunofluorescence staining. Strong signals of Arc were detected in the neuronal soma in layers 4 and 6 in the cortex (Figure 3) and these distribution patterns were consistent with those reported for Arc [28, 42] and its mRNA [51]. The immunofluorescence signals of the exogenous Luc were also detected in the neurons in layers 4 and 6 in the visual cortex (Figure 3).

Most of the immunofluorescence signals of Arc and Luc merged. From these findings, we concluded that the bioluminescence light emitted from the Tg Luc protein mimicked the expression pattern of *Arc* in the brain.

Arc is one of the neuronal immediate early gene markers in the visual cortex up-regulated by light stimuli [51]. To quantify the emitted photons from ROIs, we set a template image of the bioluminescence signals of the brain of mice under light conditions.

The ROIs including the somatosensory and visual cortex areas were selected, as shown in Figure 2, and the photon emission intensities of these regions were measured as described above.

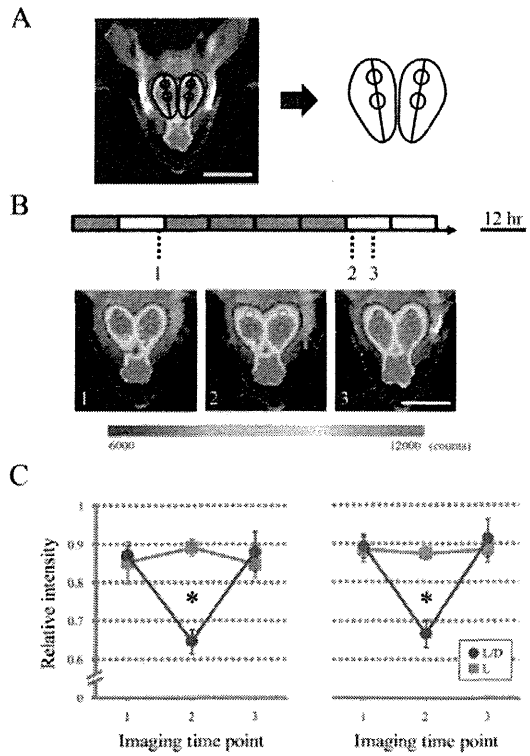

Figure 2. Changes in bioluminescence signal intensity in visual cortex of *Arc-Luc* Tg mice under light and dark conditions. A Definition of regions of interest (ROIs). A template image of bioluminescence signals of the brain under light condition was set and the ROIs including the somatosensory and visual cortex areas (circles) were identified. Then, the bioluminescence signal intensities of these regions were measured as described in the text. Scale bar, 10 mm. B Protocol for light and dark conditions and imaging (upper panel) and obtained bioluminescence images (lower panels; pseudocolored, 6000-12000 counts). The dark (gray box, 12 hr) and light (open box, 12 hr) conditions and the time points of imaging (1-3) are indicated. Imaged areas of the visual and somatosensory cortices are indicated by dotted circles. Scale bar, 10 mm. C Changes in relative bioluminescence signal intensity in visual cortex of *Arc-Luc* Tg mice (n = 14) under light (L) and dark (D) conditions (L/D). The relative intensities of bioluminescence signals in the left (left panel) and right (right panel) visual cortex regions were calculated from the measured bioluminescence signal intensity normalized with that of the somatosensory cortex. The control group of mice (n = 4) was placed under continuous light (L) condition, and bioluminescence signal intensity was measured at the same time points as those groups under L and D conditions. The data represent mean ± SD. $*p < 0.05$; two-tailed Student's *t*-test. (Modified from ref. 23 with permission).

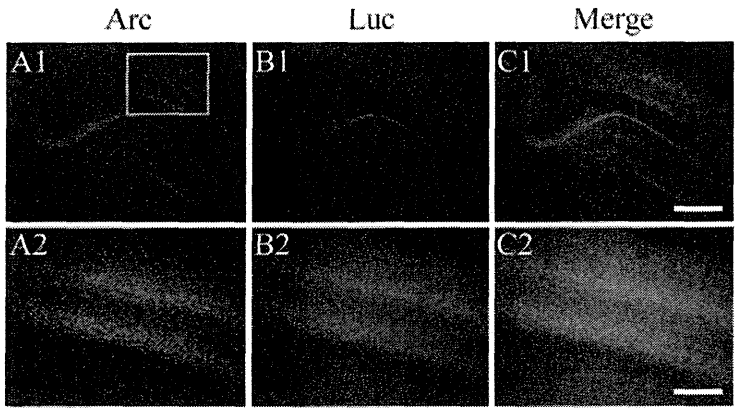

Figure 3. Distribution patterns of Arc and luciferase in visual cortex. A Immunohistochemical staining of slices with anti-Arc antibody (green, A1). Rectangles for higher-magnification images in the visual cortex (A2) are indicated in A1. B Immunofluorescence staining of the slices with anti-luciferase antibody (red, B1). Higher-magnification images of immunofluorescence signals in the visual cortex (B2). C Merged images of immunofluorescence signals of slices stained with anti-Arc and anti-luciferase antibodies (yellow, C1). Higher-magnification images of immunofluorescence signals in visual cortex (C2). Scale bar, 750 μm (A1, B1, and C1) and 300 μm (A2, B2, and C2). (Modified from ref. 23 with permission).

To examine the effect of light stimuli on the bioluminescence signals in the *Arc-Luc* Tg mice, we placed the Tg mice under dark condition for 48 hr. After this dark condition, the bioluminescence signal intensity of the posterior ROIs of the cerebral cortex apparently decreased (Figure 2).

Seven hr of continuous light exposure resulted in the recovery of the bioluminescence signal intensity in these regions (Figure 2). These regions contain the visual cortex of the mouse [8]. To evaluate quantitatively the changes in the bioluminescence signal intensity in these regions, we calculated the relative bioluminescence signal intensity in these regions in comparison with that in the central regions of the cerebral cortex containing the reported somatosensory areas of the mouse brain [4]. As shown in Figure 2, placing the mice under dark condition for 48 hr significantly decreased the bioluminescence signal intensity in the bilateral regions containing the visual cortex, which recovered after 7 hr of light exposure. Under continuous light condition, no change in relative bioluminescence signal intensity was detected (Figure 2). Furthermore, these changes in bioluminescence signal intensity correlated well with the changes in the expression levels of Arc and Luc determined by Western blot analysis. From these findings, we assume that the

Arc-Luc Tg mice are valuable for monitoring the neuronal activity in the visual cortex induced by light.

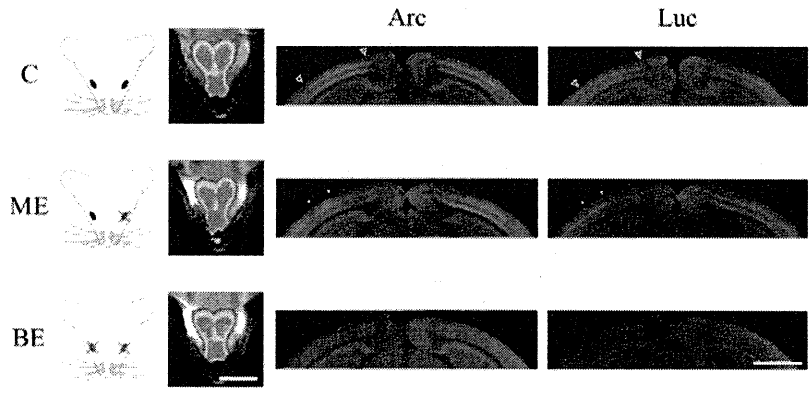

Figure 4. Changes in bioluminescence signal intensity in visual cortex of *Arc-Luc* Tg mice after visual deprivation. Illustrated figures, bioluminescence images, immunostaining of Arc (green), and immunostaining of Luc (red) of visual deprivation by eye enucleation in mice. Bioluminescence images (pseudocolored, 6000-12000 counts) were obtained over the head region of control mice before enucleation (C, upper) and after monocular enucleation (ME, middle) and binocular enucleation (BE, lower). Immunopositive signal patterns of Arc and luciferase in the visual cortex were similar to the obtained bioluminescence signal patterns in the visual cortex shown. The Arc- and Luc-positive visual cortical region is indicated by large arrowheads. The binocular visual zone is indicated by small arrowheads in ME. Scale bars, 10 mm in bioluminescence images; 2 mm in brain sections. (Modified from ref. 23 with permission).

We further confirmed the possibility that the bioluminescence signals detected in posterior brain regions correspond to the Luc expression induced by visual stimuli. The mouse visual cortex contains a large (~70%) monocular zone that receives inputs only from the contralateral eye and a small (~30%) binocular zone that receives inputs from both eyes [1]. Visual deprivation by monocular eye enucleation (ME) resulted in the significant decrease in bioluminescence signal intensity in the contralateral posterior brain region within 24 hr (Figure 4). Visual deprivation by binocular eye enucleation (BE) further decreased the bioluminescence signal intensity in the contralateral posterior brain region (Figure 4). These decreases in bioluminescence signal intensity in the posterior brain region correlated with the decreased expression levels of Arc and Luc, as revealed by immunofluorescence analyses (Figure 4). From these findings, we were able to monitor the visual-activity-dependent

changes in the bioluminescence signal intensity in the visual cortex in the *Arc-Luc* Tg mouse brain.

5. Detection of Plastic Changes in *Arc* Expression In the Visual Cortex of Adult Mice

Using *Arc-Luc* Tg mice, we detected the plastic changes in bioluminescence signal intensity after the visual deprivation in adult mice. After the ME at the age of 16 weeks, we measured the bioluminescence signal intensity in the mouse brain for three consecutive months (Figure 5). Four days after the ME, the bioluminescence signal intensity in the right visual area corresponding to the cortex contralateral to the enucleated eye decreased significantly (Figure 5).

However, one month after ME, there was no significant difference in bioluminescence signal intensity between the right and left visual areas (Figure 5). The recovered intensity of bioluminescence signals from the visual cortex contralateral to the enucleated eye was maintained for another two months. There was no obvious change in relative bioluminescence signal intensity in the ipsilateral visual cortex after ME (Figure 5).

The intensity of the bioluminescence signals obtained from both visual cortices changed equally depending on the lighting condition at latest two months after ME. These findings clearly indicate the plastic changes in *Arc-Luc* expression level in the visual cortex of the adult mouse after continuous ME.

The immediate early gene *Arc* is induced in the brain by various stimuli and is involved in synaptic plasticity during development as revealed by KO mouse studies [30, 38, 57]. Arc is considered to be involved in several forms of experience-dependent synaptic plasticity such as long-term potentiation [15], long-term depression [44], and homeostatic synaptic plasticity [47]. In the visual cortex, endogenous *Arc* expression is induced mainly in layer 4 neurons by light stimuli and is dependent on the activation of *N*-methyl-D-aspartate (NMDA) receptor channels [27, 28, 49]. The mouse visual cortex is divided into the monocular and binocular zones; in the binocular zone, the competition between the activities from inputs from both eyes continuously occurs [12].

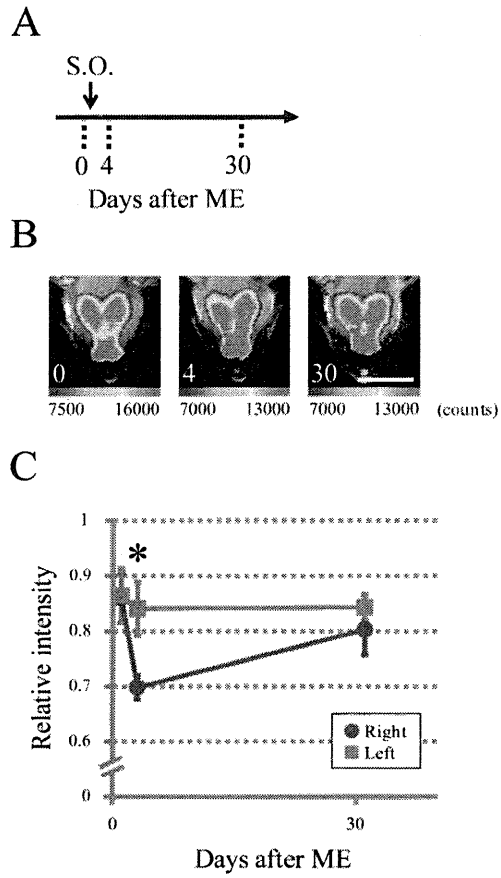

Figure 5. Detection of plastic changes in bioluminescence signal intensity in visual cortex after monocular deprivation in adult *Arc-Luc* Tg mice. A Protocol for surgical operation (S.O.) and bioluminescence imaging 0, 4, and 30 days after ME in *Arc-Luc* Tg mice. B Representative images of bioluminescence (pseudocolored, 7000-16000 counts) in visual cortex of *Arc-Luc* Tg mice taken at time points shown in A. Scale Bar, 10 mm. C Relative intensity of bioluminescence signals obtained at indicated time points shown in A. The relative intensity of bioluminescence signals in the visual cortex region is calculated in comparison with that of the somatosensory cortex. The data represent mean ± SD (n = 3-9). *$p < 0.05$; two-tailed Student's *t*-test. (Modified from ref. 23 with permission).

We detected a decrease in the bioluminescence signal intensity of Arc-Luc in the visual cortex contralateral to the enucleated eye four days after the surgery and the recovery of the signal intensity in the same area within one

month. The recovery of bioluminescence signal intensity depended on the lighting condition, at the latest two months after ME.

These findings suggest that the recovery of bioluminescence signal intensity in this visual cortex depends on the neuronal activity in the normal eye. Adult mice have a greater potential for experience-dependent plasticity than previously considered, because the MD of the dominant contralateral eye leads to a persistent, NMDA-receptor-dependent enhancement of weak ipsilateral-eye inputs [46]. Keck et al. [26] monitored by intrinsic-signal detection and two-photon imaging the functional and structural alterations in the adult mouse visual cortex after focal retinal lesioning. They suggested the activity-dependent establishment of new cortical circuits that leads to the recovery of visual responses.

On the other hand, Mrsic-Flogel et al. [32] have monitored by two-photon calcium imaging the short-term homeostatic feedback up-regulation of neuronal activity in the visual cortex after monocular deprivation. Furthermore, in the binocular zone of the adult mouse visual cortex, the extent of *Arc* induction after stimulation of the ipsilateral nondeprived eye increases and is expanded four days after ME [51]. In our study, we were unable to detect the early homeostatic up-regulation of Arc-Luc bioluminescence signals in the visual cortex four days after ME. Thus, the involvement of a homeostatic feedback process in the recovery of bioluminescence signal intensity observed one month after ME might be small. Rather, competition with neuronal-activity-dependent synaptic plasticity may be involved in the recovery process. To examine the mechanism underlying the recovery of bioluminescence signal intensity in the visual cortex contralateral to the enucleated eye, further histological examination of changes in axonal branching in the visual cortex in our ME mice is necessary.

6. Comparisons of Arc Imaging Methods

To precisely reproduce the *in vivo* expression pattern of *Arc*, we generated BAC Tg mouse strains. By homologous recombination in *E. coli* [33], we were able to precisely modify the BAC DNA containing *Arc* to insert *Luc* easily and quickly (Figure 1). The expression of large DNA transgenes such as BAC vectors can accurately reflect the transcription pattern of an endogenous chromosomal gene in a dose-dependent and integration-site-independent manner [19]. The findings of immunohistochemical and Western blot analyses using the anti-Arc and anti-luciferase antibodies supported the spatiotemporal

expression patterns of the bioluminescence signals accurately reflecting the endogenous Arc and transgenic Luc protein expression patterns. Recently, three research groups have reported the successful *in vivo* imaging of *Arc* expression by the knockin of *d2EGFP* into the *Arc* locus [57], the conventional transgenic method using the 7.1-kbp 5' upstream region of *Arc* and the fluorescent protein reporter *Venus* [10], and the BAC transgenic method using the short-life form *d4EGFP* [13] (Table 1). The reported expression patterns of *Arc-dVenus* in the visual cortex of the transgenic mice were similar to those obtained by us [23] and others [25, 51].

Table 1. Comparison of Arc-reporter mouse lines

Mouse line	Method	Promoter	Reporter	Ref.
Arc-GFP	Knockin	Endogenous	d2EGFP	57
Arc-dVenus	Conventional Tg	7.1-kb upstream	dVenus	10
TgArc/Arg3.1-d4EGFP	BAC Tg	BAC	d4EGFP	13
Arc-Luc BAC Tg	BAC Tg	BAC	Luc	23

In contrast to the superficially obtained fluorescence signals using Venus and d4EGFP [10, 13] with some autofluorescence, our results suggest that we were able to detect bioluminescence signals from the depths of the brain such as the hippocampus with a very high S/N ratio. Furthermore, bioluminescence imaging is the most sensitive method of small-animal imaging [45], and no external or cytotoxic excitation light is required to generate bioluminescence signals. We were able to perform long-term imaging of Arc-Luc expression for more than 3 months noninvasively. These features of bioluminescence imaging are suitable for the continuous monitoring and contextually relevant spatiotemporal expression of Arc in mice. In the case of our *Arc-Luc* Tg mouse strain, there are also some limitations in comparison with other *Arc*-reporter mice. Using our *Arc-Luc* Tg mouse strain, we were unable to analyze the *Arc-Luc* expression at a single-cell level *in vivo* as previously reported [13, 57]. On the other hand, a bioluminescence image could be overlaid on a photograph of a mouse used as an anatomical reference, as we showed here; however, these 2D images lack 3D information. Because algorithms have been developed to assign the position of the light source more precisely [6, 58], further analysis will reveal the source of the bioluminescence signals in the brain. In our Arc-Luc Tg mice, the temporal expression patterns of the

obtained bioluminescence signals and reported Arc protein may be slightly different, because we used wild-type firefly luciferase with a half-life of about 3 hr [52] in contrast to the endogenous Arc protein with a half-life of the about 2 hr [56, 57]. Nevertheless, despite these limitations of our mouse strain, we were able to easily monitor the neuronal-activity-dependent *Arc-Luc* expression and detected the plastic changes in *Arc* expression in the brain.

CONCLUSIONS

Bioluminescence-based imaging is a powerful method for monitoring neuronal activity in the brain. Here, we successfully generated a novel BAC Tg mouse strain, *Arc-Luc,* for monitoring the neuronal-activity-dependent *Arc* expression using bioluminescence signals in the mouse brain. Changes in bioluminescence signal intensity in the *Arc-Luc* mouse visual cortex were induced by light and dark conditions and eye enucleation.

The intensity of these bioluminescence signals correlated with endogenous Arc and exogenous Luc protein expression levels. Interestingly, we detected the recovery of bioluminescence signal intensity in the visual cortex one month after ME, suggesting the usefulness of our mouse strain for the detection of plastic changes in neuronal-activity-dependent Arc expression in the adult brain.

ACKNOWLEDGEMENTS

We thank Professor Kaoru Inokuchi for help in fluorescence microscopy and Dr. Tetsuya Ishimoto for help in bioluminescence imaging. This work was supported by a grant from the Food Safety Commission, Japan (No. 1001).

REFERENCES

[1] Antonini, A., Fagiolini, M., Stryker, M.P. (1999). Anatomical correlates of functional plasticity in mouse visual cortex. *J. Neurosci., 19,* 4388-4406.

[2] Brandes, C., Plautz, J.D., Stanewsky, R., Jamison, C.F., Straume, M., Wood, K.V., Kay, S.A., Hall, J.C. (1996). Novel features of drosophila

period transcription revealed by real-time luciferase reporting. *Neuron, 16,* 687-692.

[3] Cang, J., Kalatsky, V.A., Lowel, S., Stryker, M.P. (2005). Optical imaging of the intrinsic signal as a measure of cortical plasticity in the mouse. *Vis. Neurosci., 22,* 685-691.

[4] Caviness, V.S., Jr. (1975). Architectonic map of neocortex of the normal mouse. *J. Comp. Neurol.*, 164, 247-263.

[5] Caviness, V.S., Jr., and Frost, D.O. (1980). Tangential organization of thalamic projections to the neocortex in the mouse. *J. Comp. Neurol., 194,* 335-367.

[6] Chaudhari, A.J., Darvas, F., Bading, J.R., Moats, R.A., Conti, P.S., Smith, D.J., Cherry, S.R., Leahy, R.M. (2005). Hyperspectral and multispectral bioluminescence optical tomography for small animal imaging. *Phys. Med. Biol., 50,* 5421-5441.

[7] Chowdhury, S., Shepherd, J.D., Okuno, H., Lyford, G., Petralia, R.S., Plath, N., Kuhl, D., Huganir, R.L., Worley, P.F. (2006). Arc/Arg3.1 interacts with the endocytic machinery to regulate AMPA receptor trafficking. *Neuron, 52,* 445-459.

[8] Dräger, U.C. (1975). Receptive fields of single cells and topography in mouse visual cortex. *J. Comp. Neurol., 160,* 269-290.

[9] Dräger, U.C. (1978). Observations on monocular deprivation in mice. *J. Neurophysiol., 41,* 28-42.

[10] Eguchi, M., and Yamaguchi, S. (2009). In vivo and in vitro visualization of gene expression dynamics over extensive areas of the brain. *NeuroImage, 44,* 1274-1283.

[11] Frenkel, M.Y., and Bear, M.F. (2004). How monocular deprivation shifts ocular dominance in visual cortex of young mice. *Neuron, 44,* 917-923.

[12] Gordon, J.A., and Stryker, M.P. (1996). Experience-dependent plasticity of binocular responses in the primary visual cortex of the mouse. *J. Neurosci., 16,* 3274-3286.

[13] Grinevich, V., Kolleker, A., Eliava, M., Takada, N., Takuma, H., Fukazawa, Y., Shigemoto, R., Kuhl, D., Waters, J., Seeburg, P.H., Osten, P. (2009). Fluorescent Arc/Arg3.1 indicator mice: a versatile tool to study brain activity changes in vitro and in vivo. *J. Neurosci. Methods,* 184, 25-36.

[14] Guzowski, J.F., McNaughton, B.L., Barnes, C.A., Worley, P.F. (1999). Environment-specific expression of the immediate-early gene Arc in hippocampal neuronal ensembles. *Nat. Neurosci., 2,* 1120-1124.

[15] Guzowski, J.F., Lyford, G.L., Stevenson, G.D., Houston, F.P., McGaugh, J.L., Worley, P.F., Barnes, C.A. (2000). Inhibition of activity-dependent arc protein expression in the rat hippocampus impairs the maintenance of long-term potentiation and the consolidation of long-term memory. *J. Neurosci., 20,* 3993-4001.

[16] Guzowski, J.F., Setlow, B., Wagner, E.K., McGaugh, J.L. (2001). Experience-dependent gene expression in the rat hippocampus after spatial learning: a comparison of the immediate-early genes Arc, c-fos, and zif268. *J. Neurosci., 21,* 5089-5098.

[17] Guzowski, J.F., Knierim, J.J., Moser, E.I. (2004). Ensemble dynamics of hippocampal regions CA3 and CA1. *Neuron,* 44, 581-584.

[18] Heimel, J.A., Hartman, R.J., Hermans, J.M., Levelt, C.N. (2007). Screening mouse vision with intrinsic signal optical imaging. *Eur. J. Neurosci., 25,* 795-804.

[19] Heintz, N. (2001). BAC to the future: the use of bac transgenic mice for neuroscience research. *Nat. Rev. Neurosci., 2,* 861-870.

[20] Hensch, T.K., Fagiolini, M., Mataga, N., Stryker, M.P., Baekkeskov, S., Kash, S.F. (1998). Local GABA circuit control of experience-dependent plasticity in developing visual cortex. *Science, 282,* 1504-1508.

[21] Hofer, S.B., Mrsic-Flogel, T.D., Bonhoeffer, T., Hubener, M. (2006). Prior experience enhances plasticity in adult visual cortex. *Nat. Neurosci., 9,* 127-132.

[22] Huang, Z.J., Kirkwood, A., Pizzorusso, T., Porciatti, V., Morales, B., Bear, M.F., Maffei, L., Tonegawa, S. (1999). BDNF regulates the maturation of inhibition and the critical period of plasticity in mouse visual cortex. *Cell, 98,* 739-755.

[23] Izumi, H., Ishimoto, T., Yamamoto, H., Nishijo, H., Mori, H. (2011). Bioluminescence imaging of Arc expression enables detection of activity-dependent and plastic changes in the visual cortex of adult mice. *Brain Struct. Funct., 216,* 91-104.

[24] Kalatsky, V.A., and Stryker, M.P. (2003). New paradigm for optical imaging: temporally encoded maps of intrinsic signal. *Neuron, 38,* 529-545.

[25] Kawashima, T., Okuno, H., Nonaka, M., Adachi-Morishima, A., Kyo, N., Okamura, M., Takemoto-Kimura, S., Worley, P.F., Bito, H. (2009). Synaptic activity-responsive element in the Arc/Arg3.1 promoter essential for synapse-to-nucleus signaling in activated neurons. *Proc. Natl. Acad. Sci. USA., 106,* 316-321.

[26] Keck, T., Mrsic-Flogel, T.D., Vaz Afonso, M., Eysel, U.T., Bonhoeffer, T., Hübener, M. (2008). Massive restructuring of neuronal circuits during functional reorganization of adult visual cortex. *Nat. Neurosci., 11,* 1162-1167.

[27] Link, W., Konietzko, U., Kauselmann, G., Krug, M., Schwanke, B., Frey, U., Kuhl, D. (1995). Somatodendritic expression of an immediate early gene is regulated by synaptic activity. *Proc. Natl. Acad. Sci. USA., 92,* 5734-5738.

[28] Lyford, G.L., Yamagata, K., Kaufmann, W.E., Barnes, C.A., Sanders, L.K., Copeland, N.G., Gilbert, D.J., Jenkins, N.A., Lanahan, A.A., Worley, P.F. (1995). Arc, a growth factor and activity-regulated gene, encodes a novel cytoskeleton-associated protein that is enriched in neuronal dendrites. *Neuron, 14,* 433-445.

[29] Martin, J.R. (2008). In vivo brain imaging: Fluorescence or bioluminescence, which to choose? *J. Neurogenet., 22,* 285-307.

[30] McCurry, C.L., Shepherd, J.D., Tropea, D., Wang, K.H., Bear, M.F., Sur, M. (2010). Loss of Arc renders the visual cortex impervious to the effects of sensory experience or deprivation. *Nat. Neurosci., 13,* 450-457.

[31] Metin, C., Godement, P., Imbert, M. (1988). The primary visual cortex in the mouse: receptive field properties and functional organization. *Exp. Brain Res.,* 69, 594-612.

[32] Mrsic-Flogel, T.D., Hofer, S.B., Ohki, K., Reid, R.C., Bonhoeffer, T., Hübener, M. (2007). Homeostatic regulation of eye-specific responses in visual cortex during ocular dominance plasticity. *Neuron, 54,* 961-972.

[33] Muyrers, J.P., Zhang, Y., Testa, G., Stewart, A.F. (1999). Rapid modification of bacterial artificial chromosome by ET-recombination. *Nucleic Acids Res., 27,* 1555-1557.

[34] Ohki, K., Chung, S., Ch'ng, Y.H., Kara, P., Reid, R.C. (2005). Functional imaging with cellular resolution reveals precise micro-architecture in visual cortex. *Nature, 433,* 597-603.

[35] Okuno, H. (2011). Regulation and function of immediate-early genes in the brain: beyond neuronal activity markers. *Neurosci. Res., 69,* 175-186.

[36] Olavarria, J. and Montero, V.M. (1989). Organization of visual cortex in the mouse revealed by correlating callosal and striate-extrastriate connections. *Vis. Neurosci., 3,* 59-69.

[37] Pham, T.A., Graham, S.J., Suzuki, S., Barco, A., Kandel, E.R., Gordon, B., Lickey, M.E. (2004). A semi-persistent adult ocular dominance

plasticity in visual cortex is stabilized by activated CREB. *Learn. Mem., 11,* 738-747.

[38] Plath, N., Ohana, O., Dammermann, B., Errington, M.L., Schmitz, D., Gross, C., Mao, X., Engelsberg, A., Mahlke, C., Welzl, H., Kobalz, U., Stawrakakis, A., Fernandez, E., Waltereit, R., Bick-Sander, A., Therstappen, E., Cooke, S.F., Blanquet, V., Wurst, W., Salmen, B., Bösl, M.R., Lipp, H.P., Grant, S.G., Bliss, T.V., Wolfer, D.P., Kuhl, D. (2006). Arc/Arg3.1 is essential for the consolidation of synaptic plasticity and memories. *Neuron, 52,* 437-444.

[39] Porciatti, V., Pizzorusso, T., Maffei, L. (1999). The visual physiology of the wild type mouse determined with pattern VEPs. *Vision Res., 39,* 3071-3081.

[40] Prescher, J.A., and Contag, C.H. (2010). Guided by the light: visualizing biomolecular processes in living animals with bioluminescence. *Curr. Opin. Chem. Biol.,* 14, 80-89.

[41] Prusky, G.T., West, P.W., Douglas, R.M. (2000). Behavioral assessment of visual acuity in mice and rats. *Vision Res., 40,* 2201-2209.

[42] Ramirez-Amaya, V., Vazdarjanova, A., Mikhael, D., Rosi, S., Worley, P.F., Barnes, C.A. (2005). Spatial exploration-induced Arc mRNA and protein expression: evidence for selective, network-specific reactivation. *J. Neurosci., 25,* 1761-1768.

[43] Regehr, W.G., and Tank, D.W. (1991). Selective fura-2 loading of presynaptic terminals and nerve cell processes by local perfusion in mammalian brain slice. *J. Neurosci. Methods, 37,* 111-119.

[44] Rial Verde, E.M., Lee-Osbourne, J., Worley, P.F., Malinow, R., Cline, H.T. (2006). Increased expression of the immediate-early gene arc/arg3.1 reduces AMPA receptor-mediated synaptic transmission. *Neuron, 52,* 461-474.

[45] Rice, B.W., Cable, M.D., Nelson, M.B. (2001). In vivo imaging of light-emitting probes. *J. Biomed. Opt.,* 6, 432-440.

[46] Sawtell, N.B., Frenkel, M.Y., Philpot, B.D., Nakazawa, K., Tonegawa, S., Bear, M.F. (2003). NMDA receptor-dependent ocular dominance plasticity in adult visual cortex. *Neuron, 38,* 977-985.

[47] Shepherd, J.D., Rumbaugh, G., Wu, J., Chowdhury, S., Plath, N., Kuhl, D., Huganir, R.L., Worley, P.F. (2006). Arc/Arg3.1 mediates homeostatic synaptic scaling of AMPA receptors. *Neuron, 52,* 475-484.

[48] Simmons, P.A., Lemmon, V., Pearlman, A.L. (1982). Afferent and efferent connections of the striate and extrastriate visual cortex of the normal and reeler mouse. *J. Comp. Neurol., 211,* 295-308.

[49] Steward, O., and Worley, P.F. (2001). Selective targeting of newly synthesized Arc mRNA to active synapses requires NMDA receptor activation. *Neuron, 30,* 227-240.

[50] Stosiek, C., Garaschuk, O., Holthoff, K., Konnerth, A. (2003). In vivo two-photon calcium imaging of neuronal networks. *Proc. Natl. Acad. Sci. USA., 100,* 7319-7324.

[51] Tagawa, Y., Kanold, P.O., Majdan, M., Shatz, C.J. (2005). Multiple periods of functional ocular dominance plasticity in mouse visual cortex. *Nat. Neurosci., 8,* 380-388.

[52] Thompson, J.F., Hayes, L.S., Lloyd, D.B. (1991). Modulation of firefly luciferase stability and impact on studies of gene regulation. *Gene, 103,* 171-177.

[53] Tropea, D., Van Wart, A., Sur, M. (2009). Molecular mechanisms of experience-dependent plasticity in visual cortex. *Phil. Trans. R. Soc. B, 364,* 341-355.

[54] Vazdarjanova, A., and Guzowski, J.F. (2004). Differences in hippocampal neuronal population responses to modifications of an environmental context: evidence for distinct, yet complementary, functions of CA3 and CA1 ensembles. *J. Neurosci., 24,* 6489-6496.

[55] Wagor, E., Mangini, N.J., Pearlman, A.L. (1980). Retinotopic organization of striate and extrastriate visual cortex in the mouse. *J. Comp. Neurol., 193,* 187-202.

[56] Wallace, C.S., Lyford, G.L., Worley, P.F., Steward, O. (1998). Differential intracellular sorting of immediate early gene mRNAs depends on signals in the mRNA sequence. *J. Neurosci., 18,* 26-35.

[57] Wang, K.H., Majewska, A., Schummers, J., Farley, B., Hu, C., Sur, M., Tonegawa, S. (2006). In vivo two-photon imaging reveals a role of Arc in enhancing orientation specificity in visual cortex. *Cell, 126,* 389-402.

[58] Wang, G., Cong, W., Shen, H., Qian, X., Henry, M., Wang, Y. (2008). Overview of bioluminescence tomography-a new molecular imaging modality. *Front. Biosci., 13,* 1281-1293.

[59] Wang, Q., and Burkhalter, A. (2007). Area map of mouse visual cortex. *J. Comp. Neurol., 502,* 339-357.

RESEARCH ARTICLE

AMERICAN JOURNAL OF medical genetics PART A

Clinical and Radiological Features of Japanese Patients With a Severe Phenotype due to *CASK* Mutations

Jun-ichi Takanashi,[1,2]* Nobuhiko Okamoto,[3] Yuto Yamamoto,[3] Shin Hayashi,[4] Hiroshi Arai,[5] Yukitoshi Takahashi,[6] Koichi Maruyama,[7] Seiji Mizuno,[7] Shuichi Shimakawa,[8] Hiroaki Ono,[9] Reiki Oyanagi,[10] Satomi Kubo,[11] A. James Barkovich,[12] and Johji Inazawa[4]

[1]Department of Pediatrics, Kameda Medical Center, Kamogawa, Japan

[2]Department of Radiology, Toho University Sakura Medical Center, Sakura, Japan

[3]Department of Medical Genetics, Osaka Medical Center and Research Institute for Maternal and Child Health, Osaka, Japan

[4]Department of Molecular Cytogenetics, Medical Research Institute and School of Biomedical Science, Tokyo Medical and Dental University, Tokyo, Japan

[5]Department of Pediatric Neurology, Morinomiya Hospital, Osaka, Japan

[6]National Epilepsy Center, Shizuoka Institute of Epilepsy and Neurological Disorders, Shizuoka, Japan

[7]Department of Pediatric Neurology, Aichi Prefectural Colony Central Hospital, Kasugai, Japan

[8]Department of Pediatrics, Osaka Medical College, Takatsuki, Japan

[9]Department of Pediatrics, Hiroshima Prefectural Hospital, Hiroshima, Japan

[10]Department of Pediatrics, Hokkaido Medical Center for Child Health and Rehabilitation, Sapporo, Japan

[11]Department of Pediatrics, Nara Prefectural Nara Hospital, Nara, Japan

[12]Department of Radiology and Biomedical Imaging, University of California San Francisco, California

Manuscript Received: 31 March 2012; Manuscript Accepted: 5 August 2012

Heterozygous loss of function mutations of *CASK* at Xp11.4 in females cause severe intellectual disability (ID) and microcephaly with pontine and cerebellar hypoplasia (MICPCH). However, the longitudinal clinical and radiological course of affected patients, including patterns of postnatal growth, has not been described. Neurodevelopmental and imaging information was retrospectively accrued for 16 Japanese (15 female and 1 male) patients with ID and MICPCH associated with *CASK* mutations. All records were analyzed; patient age ranged from 2 to 16 years at the time of the most recent examinations. The growth pattern, neurological development, neurological signs/symptoms, and facial features were similar in the 15 female patients. Their head circumference at birth was within the normal range in about half, and their height and weight were frequently normal. This was followed by early development of severe microcephaly and postnatal growth retardation. The patients acquired head control almost normally between 3 and 6 months, followed by motor delay. More than half of the female patients had epilepsy. Their MRIs showed microcephaly, brainstem, and cerebellar hypoplasia in early infancy, and a normal or large appearing corpus callosum. The male patient showed a more severe clinical phenotype. These uniform clinical and radiological features should facilitate an early diagnosis and be useful for medical care of females with ID and MICPCH associated with *CASK* mutations.

How to Cite this Article:
Takanashi J-i, Okamoto N, Yamamoto Y, Hayashi S, Arai H, Takahashi Y, Maruyaa K, Mizuno S, Shimakawa S, Ono H, Oyanagi R, Kubo S, Barkovich AJ, Inazawa J. 2012. Clinical and radiological features of Japanese patients with a severe phenotype due to *CASK* mutations.
Am J Med Genet Part A 158A:3112–3118.

Grant sponsor: Research Grant for Nervous and Mental Disorders, Ministry of Health, Labor and Welfare of Japan; Grant number: 24-7; Grant sponsor: Grant-in-Aid for Scientific Research (C), JSPS; Grant number: 24591790; Grant sponsor: Health and Labor Sciences Research Grants, Ministry of Health, Labor and Welfare of Japan; Grant sponsor: New Energy and Industrial Technology Development Organization (NEDO).
The authors declared that they have no conflicts of interest.
*Correspondence to:
Jun-ichi Takanashi, Department of Pediatrics, Kameda Medical Center, 929 Higashi-cho, Kamogawa-shi, Chiba 296-8602, Japan.
E-mail: jtaka44@hotmail.co.jp
Article first published online in Wiley Online Library (wileyonlinelibrary.com): 19 November 2012
DOI 10.1002/ajmg.a.35640

Key words: *CASK*; Intellectual disability; microcephaly; pontine hypoplasia; cerebellar hypoplasia; epilepsy; MRI

INTRODUCTION

The CASK protein belongs to the membrane-associated guanylate kinase protein family, functioning as a multi-domain scaffolding protein, and plays important roles in neural development and synaptic function [Hsueh, 2006, 2009; Hayashi et al., 2008; Najm et al., 2008]. It has been reported that *CASK* aberrations can cause three clinical phenotypes, severe intellectual disability (ID) and microcephaly with pontine and cerebellar hypoplasia (MICPCH, OMIM: #300749) in females [Takanashi et al., 2010; Moog et al., 2011; Hayashi et al., 2012], mild to severe ID with or without nystagmus, microcephaly, and/or dysmorphic features in males [Hackett et al., 2010], and FG syndrome in males [Piluso et al., 2009] depending on the type of aberration of the gene [Moog et al., 2011; Hayashi et al., 2012]. Hypomorphic missense mutations of *CASK* in males probably cause FG syndrome or mild to severe ID with or without nystagmus, microcephaly, and/or dysmorphic features, whereas *CASK* null mutations (haploinsufficiency of *CASK*) in females cause ID and MICPCH [Moog et al., 2011; Hayashi et al., 2012]. This theory explains the similarity of the clinical and radiological phenotypes of ID and MICPCH regardless of the type of *CASK* mutation [Takanashi et al., 2010; Moog et al., 2011; Hayashi et al., 2012]; however, no long-term clinical and radiological information has been published on this group of patients. We present clinical and radiological evaluations of 16 Japanese patients with ID and MICPCH associated with *CASK* mutations.

MATERIALS AND METHODS

Sixteen Japanese patients (15 female and 1 male, 2–16 years old) clinically diagnosed with ID and MICPCH and confirmed to have *CASK* mutations were enrolled in this study. Written informed consent for genetic and clinical analysis was obtained from the parents after institutional review board approval was obtained from Tokyo Medical and Dental University and Kameda Medical Center. Genetic analysis and brief clinical features of 10 of the 16 patients [Hayashi et al., 2012], and magnetic resonance imaging (MRI) features of 5 of the 16 patients [Takanashi et al., 2010] were previously reported, respectively. The 15 female patients most likely have *CASK* loss-of-function mutations [Hayashi et al., 2012], which are expected to cause a characteristic pattern of ID and MICPCH in females [Moog et al., 2011; Hayashi et al., 2012]. In silico prediction programs and splice site prediction software showed that the de novo mutation in a male (Patient 16), situated in an important interaction domain of CASK, was considered to damaging to protein function, and this position was not associated with a splice site. We reviewed all available data, including MRI scans, raw data from the MRIs for use in quantification, and information concerning growth, development, and neurologic status. Height, weight, and head circumference were measured in all patients at birth, and subsequently recorded two to five times for female patients, and six times for the male. The MRI data with 1.5 T magnet were used to quantify the area of the cerebrum, cerebellar hemispheres, pons, and corpus callosum in each patient using the same methods previously reported [Takanashi et al., 2010]; patients ranged in age from 4 to 156 months at the time of their MRI. One (Patient 11) was scanned three times at ages 9, 24, and 50 months. The results of these measurements were compared with those of 62 female patients (0.5–180 months old) evaluated at the Kameda Medical Center using 1.5 T Siemens apparatus for mild neurological symptoms, such as headache, hypotonia, seizures, febrile delirium, or mild asphyxia, who had no parenchymal lesion on MRI, and showed normal subsequent neurodevelopmental exams; as well as those of five patients with pontine hypoplasia due to causes other than *CASK* mutations, including PEHO [Tanaka et al., 1997], 5p-syndrome [Ninchoji and Takanashi, 2010], and trisomy 18 (disease controls).

RESULTS

Clinical Records

The epilepsy and genetic data of the 16 patients with ID and MICPCH associated with *CASK* mutations are summarized in Table I. Postnatal growth curves are shown in Figure 1 (head circumference in Fig. 1a; height and weight in Fig. 1b,c). Fifteen patients were born at term (>37 weeks gestation); mean OFC was 30.4 ± 1.7 (mean $\pm$ SD) cm, height was 47.0 ± 2.6 cm, and weight was 2640 ± 420 g. Patient 5 was born at 33 weeks' gestation with an OFC of 28.0 cm, height of 41.4 cm, weight of 1596 g. Microcephaly, defined as less than the third centile (30.2 cm), was present at birth in 7/15 (47%) patients born at term. Microcephaly was recognized in all patients examined after age 4 months, with OFC measuring below −4 SD, including a male patient (Fig. 1, stars) and a female born at 33 weeks. Height at birth was low normal (within 2 SD) in 13/15 patients born at term, declining to around the −2 SD level after 4 years, and below the −3 SD level after 8 years. Birth weight was normal or low normal in 14/15 patients born at term, decreasing to the −1 SD to −2 SD level after 4 months, and around the −2 SD after 2 years. Height and weight of a male patient (Fig. 1, stars) and a female born at 33 weeks overlapped those of females born at term.

Hypotonia was observed in 11/16, muscle weakness in 10/16, spasticity or increased deep tendon reflexes in 12/16, involuntary movements in 3/16, sensory deafness in 2/16, and ophthalmologic anomalies in 3/16 (abnormal visual evoked potentials, strabismus, and nystagmus), respectively. Four patients presented with hypohidrosis, and two of these also showed hyposensitivity to pain. A typical facial appearance (Fig. 2) was noted (including the male patient, Fig. 2b), with an oval face in all patients, large eyes, or irises in 13/16, large ears in 11/16, a broad nasal bridge in 14/16, a broad nasal tip in 9/16, a small nose in 6/16, epicanthal folds in 5/16, a small jaw in 11/16, a long philtrum in 7/16, and a high-arched palate in 7/16.

The motor milestones are shown in Figure 3. The male (Patient 16) showed no psychomotor development at 5 years old, that is, he could not control his head, smile, or babble. The 15 female patients exhibited early psychomotor development; all